

- ¹K. P. Belov, A. K. Zvezdin, R. Z. Levitin, A. S. Markosyan, B. V. Mill', A. A. Mukhin, and A. P. Perov, *Zh. Eksp. Teor. Fiz.* **68**, 1189 (1975) [*Sov. Phys. JETP* **41**, 590 (1975)].
- ²V. D. Doroshev, S. F. Ivanov, M. M. Koftun, and V. M. Selez'ob, *Dopovidi AN URSSR*, No. 1, 68 (1973).
- ³E. A. Turov and M. P. Petrov, *Yaderniy magnitnyy rezonans v ferro- i antiferromagnetnikakh* (Nuclear Magnetic Resonance in Ferro- and Antiferromagnets), Nauka, 1969.
- ⁴R. L. Streever and P. J. Caplan, *Phys. Rev. [B]* **4**, 2881 (1971).
- ⁵C. Robert and F. Hartmann-Boutron, *J. Phys. Radium* **23**, 574 (1962).
- ⁶V. G. Bar'yakhtar, V. A. Klochan, N. M. Kovtun, and E. E. Solov'ev, *Fiz. Tverd. Tela* **16**, 2058 (1974) [*Sov. Phys. Solid State* **16**, 1236 (1975)].
- ⁷K. P. Belov, A. K. Gapeev, R. Z. Levitin, A. S. Markosyan, and Yu. F. Popov, *Zh. Eksp. Teor. Fiz.* **68**, 241 (1975) [*Sov. Phys. JETP* **41**, 117 (1975)].
- ⁸A. S. Markosyan, Author's abstract of dissertation for the degree of Candidate of Physical and Mathematical Sciences, Moscow State University, 1975.
- ⁹V. G. Demidov, A. K. Zvezdin, R. Z. Levitin, A. S. Markosyan, and A. I. Popov, *Fiz. Tverd. Tela* **16**, 2114 (1974) [*Sov. Phys. Solid State* **16**, 1379 (1975)].
- ¹⁰V. G. Bar'yakhtar, A. E. Borovik, and V. A. Popov, *Pis'ma Zh. Eksp. Teor. Fiz.* **9**, 634 (1969) [*JETP Lett.* **9**, 391 (1969)].
- ¹¹V. G. Bar'yakhtar, A. E. Borovik, V. A. Popov, and E. P. Stefanovskii, *Zh. Eksp. Teor. Fiz.* **59**, 1299 (1970) [*Sov. Phys. JETP* **32**, 709 (1971)].
- ¹²A. I. Mitsek, N. P. Kolmakova, and P. F. Gaïdanskii, *Fiz. Tverd. Tela* **11**, 1258 (1969) [*Sov. Phys. Solid State* **11**, 1021 (1969)].
- ¹³A. I. Mitsek and P. F. Gaïdanskii, *Phys. Status Solidi [a]* **4**, 319 (1971).
- ¹⁴M. Shirobokov, *Zh. Eksp. Teor. Fiz.* **15**, 57 (1945).
- ¹⁵J. F. Dillon, *J. Appl. Phys.* **29**, 539 (1968).
- ¹⁶V. D. Dylgerov and A. I. Drokin, *Kristallografiya* **5**, 945 (1960) [*Sov. Phys. Crystallogr.* **5**, 900 (1961)].
- ¹⁷J. R. Patel, K. A. Jackson, and J. F. Dillon, *J. Appl. Phys.* **39**, 3767 (1968).
- ¹⁸J. E. Kunzler, L. R. Walker, and J. K. Galt, *Phys. Rev.* **119**, 1609 (1960).
- ¹⁹S. S. Shinozaki, *Phys. Rev.* **122**, 388 (1961).
- ²⁰V. K. Vlasko-Vlasov, L. M. Dedukh, and V. I. Nikitenko, *Zh. Eksp. Teor. Fiz.* **65**, 376 (1973) [*Sov. Phys. JETP* **38**, 184 (1974)].

Translated by J. G. Adashko

Equivalent noncollinear structures in the cubic ferrimagnet GdIG induced by a magnetic field

S. L. Gnatchenko and N. F. Kharchenko

Physico-technical Institute of Low Temperatures, Ukrainian Academy of Sciences

(Submitted October 9, 1975)

Zh. Eksp. Teor. Fiz. **70**, 1379-1393 (April 1976)

Fracture of GdIG sublattices near T_c is studied by means of the Faraday magneto-optical effect. A transverse experimental geometry is used, in which the light-propagation vector \mathbf{k} is perpendicular to \mathbf{H} . The coexistence of noncollinear equivalent magnetic structures (magnetic twins) is observed visually. The magnetic diagrams of the GdIG states are plotted on the basis of the observations for the cases $\mathbf{H} \parallel [100]$ and $\mathbf{H} \parallel [111]$. They are in satisfactory agreement with calculations performed within the framework of the molecular-field approximation with allowance for the GdIG three-sublattice structure and cubic anisotropy. It is suggested that the tail observed on the $\Phi(T)$ curve with increasing distance from the phase-transition line in the case of $\mathbf{H} \parallel [100]$ is due to microscopic defects of the sample and is similar to the tail of the technical-magnetization curve at saturation.

PACS numbers: 75.25.+z, 75.30.Gw, 78.20.Ls

A sufficiently strong field applied to a collinear ferrimagnet upsets the parallelism of its sublattices (see^[1], where references to earlier work are given). For a number of reasons (stratification near first-order phase transitions, the presence of several equivalent directions), the resultant noncollinear structure cannot be homogeneous. Visual observation of an inhomogeneous noncollinear magnetic structure of rare-earth iron garnets was reported in^[2-5]. The results of the investigation of the stratification of the magnetic phases in the vicinities of first-order orientational transitions in gadolinium iron garnets were discussed in^[4,5]. In this paper we investigate the twinning of the field-induced magnetic noncollinear structure of a gadolinium iron garnet when the magnetic field is ordered along its high-order symmetry axes.

METHODOLOGICAL REMARKS

The experimental method used was based on the magneto-optical rotation of the polarization plane whereby, owing to the significantly different partial contributions of the individual sublattices of the GdIG, it becomes possible to determine the angle between the magnetic moment of the optically active sublattice and the light-propagation direction. We used a transverse experimental geometry, in which the light-propagation direction \mathbf{k} was perpendicular to the magnetic field \mathbf{H} . At the employed field strengths, the angles between the magnetic moments of the a and d sublattices differ very little from 180° , and, neglecting the small contributions to the Faraday rotation of the GdIG, we can write

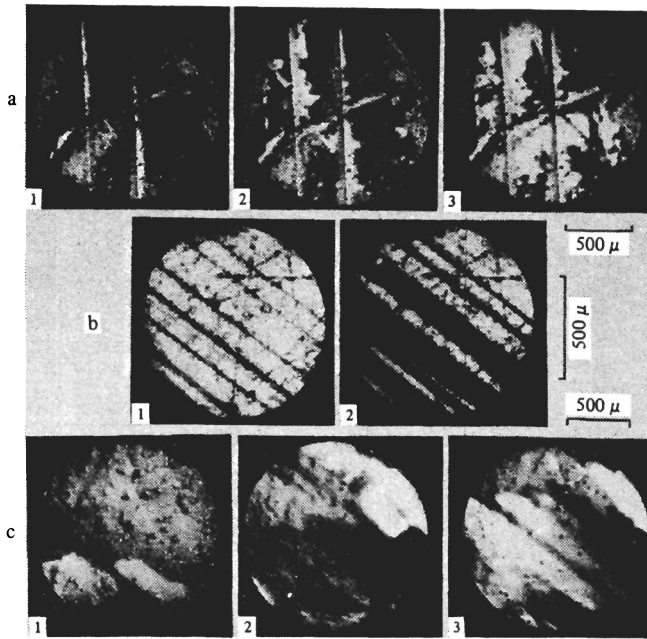


FIG. 1. Characteristic domains pictures observed in gadolinium iron garnet plates at temperatures close to T_c . The magnetic field is directed along the advanced plane of the plate. a) Sample with mechanically polished surfaces: 1— $T = 278.2$ K, 2— 278.8 K, 3— 279.9 K; $T_c = 279.5$ K, $H = 14$ kOe. b) Sample cut from crystal with noticeable growth traces, surfaces mechanically polished: 1— $T = 284.0$ K, 2— 283.7 K; $T_c \approx 282$ K, $H = 14.3$ kOe. c) Heat-treated sample with chemically polished surfaces: 1— $T = 278.4$ K, 2— 280.3 K, 3— 280.7 K; $T_c \approx 279.5$ K, $H = 13.8$ kOe.

$$\Phi = \Phi_0 \sin \theta \cos \varphi,$$

where Φ_0 is the spontaneous rotation, $\theta \approx \theta_a \approx \theta_d$ is the angle between the directions of the magnetic moment of the iron (a or d) sublattice and the collinear ($\mathbf{M}_i \parallel \mathbf{H}$) and canted phases, and φ is the azimuthal angle reckoned from the $x \parallel \mathbf{k}$ axis. The transverse geometry makes it possible to distinguish between energywise equivalent magnetic states characterized by the same rotation angles of the sublattice moments relative to the vector \mathbf{H} , but by different azimuthal angles of the moments.

The usual optical scheme for the observation of magnetic domains with the aid of the Faraday effect was supplemented with a recording system in which the light beam was modulated in the polarization plane. A mirror-diaphragm with dimensions corresponding to the a sample region of approximate diameter 75μ was placed in the image plane. The light which did not pass through the diaphragm was reflected from the mirror and passed through an analyzer into an eyepiece with which it was possible, simultaneously with the measurements, to monitor visually the position of the diaphragm relative to the domain image. For the visual observation we used the white light of an incandescent lamp; its advantage over monochromatic light was that the dispersion curves of the absorption and of the Faraday rotation were different. Competition between these two properties leads to the appearance of a colored domain picture. The domain color depends on the

angle between the vectors \mathbf{M}_a and \mathbf{k} and on the analyzer positions. The color hues are of great help in the visual identification and tracing the behavior of the domains of the various magnetic phases.

The gadolinium iron garnet samples were cut in the form of plates oriented in the (110) plane. After mechanical polishing, the plate thickness ranged from 30 to 50μ . The plates were annealed in an oxygen atmosphere at 1000 – 1100°C and were chemically polished in orthophosphoric acid. The sample was freely placed in a copper capsule placed inside a cell with the heat-exchange gas; the capsule could be rotated about the horizontal axis ($\parallel \mathbf{k}$ and $\perp \mathbf{H}$) and the vertical axis ($\perp \mathbf{k}$, $\perp \mathbf{H}$). The directions of the crystallographic axes were determined by x-ray diffraction. In addition, further adjustment and monitoring were effected by observing the walls of the ordinary magnetic domains far from T_c at low field intensities (up to 100 Oe), and also by attaining symmetry of the Faraday rotation relative to small rotations of the sample, under the condition that the latter is in a noncollinear state (near the boundary between existence of the collinear and canted phases). The adjustment error did not exceed 1 – 2° .

The sample temperature could be maintained constant accurate to $\pm 0.01^\circ\text{K}$ or varied smoothly at rates from 10^{-3} to 10^{-2} K/sec in the interval from 200 to 350 K. To measure the temperature we used copper-constantan thermocouples. The absolute measurement error is estimated by us at about 0.2°K . The temperature gradient at the sample was monitored by various means and did not exceed $0.01^\circ\text{K}/\text{mm}$. To prevent heating of the sample by light, the thickness of the thermal filter was chosen such that its further increase did not influence the domain configuration in all the investigated intervals of the magnetic field and temperatures.

EXPERIMENTAL RESULTS

Visual observations in polarized light have shown that a gadolinium iron garnet sample placed in a magnetic field becomes magnetically-inhomogeneous when its temperature approaches the magnetic-compensation temperature. The position of the boundaries of the inhomogeneous-state region depend somewhat on the orientation of the magnetic field relative to the crystallographic directions. The temperature interval of the existence of the domain structure increases with increasing field intensity, starting with fields of several kOe. At $H = 14$ kOe, this interval is approximately 3°K . The form of the domain picture depends essentially on the surface state of the sample, its thermal prior history, and the growth conditions.

Figure 1 shows photographs of the observed characteristic domain pictures of certain samples. In the mechanically-polished surfaces (Fig. 1a) the domains usually appear near the surface defects. Samples cut from crystals with noticeable growth directions are characterized by a strip domain structure with strips parallel to growth traces (Fig. 1b). The domain picture of the chemically polished samples varied with time over one month.

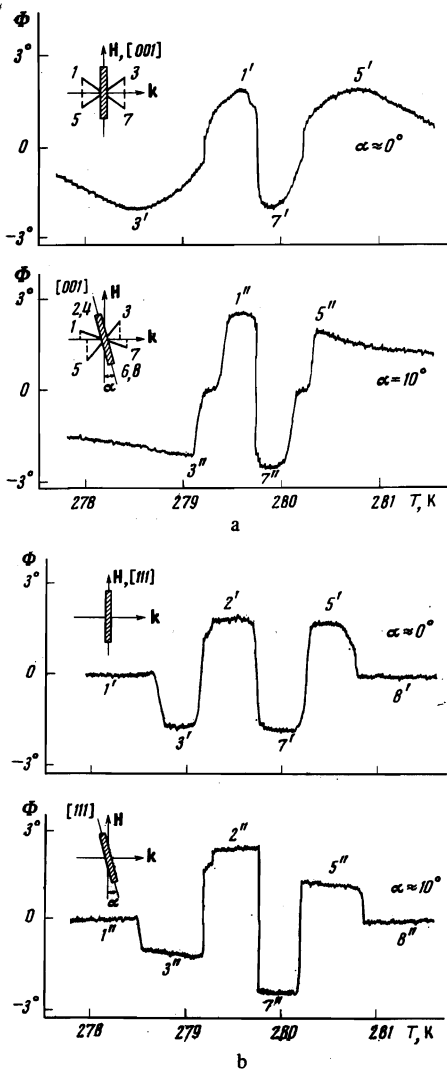


FIG. 2. Faraday rotation in a sample section of 75μ diameter in following cases: a) direction of H is close to the [100] axis, b) direction of H is close to the [111] axis. In both cases $H=13.8$ kOe.

Although the observed domain pictures were different, the temperature intervals within which the magnetic state is inhomogeneous changed little from sample to sample. This circumstance, together with the high sensitivity of the form of the domain picture to the orientation of the magnetic field, and also the existence of well pronounced easily mobile domain walls offer evidence that the formation of the domain structure is due to the appearance, near T_c , of several energywise stable magnetic states, and is connected to a much lesser degree with the inhomogeneity of the compensation temperature over the sample.

The investigated samples contained at times blocks characterized by values of T_c different from the compensation temperature of the remainder of the sample by several tenths of a degree $^{\circ}\text{K}$. These are not noticeable in the domain structure of a chemically polished sample far from T_c , but in the immediate vicinity of T_c and in the presence of a magnetic field the blocks are clearly pronounced. The results reported below per-

tain either to samples with many blocks or to individual blocks.

The observed domain pictures are quite difficult to identify, owing to the presence of domain walls parallel to the advanced surface of the sample. Slight deviations of the vector H from a high-symmetry axis decreases the number of parallel walls, and at an inclination angle of about 3° the domains already penetrate all the way through the sample. By using a recording system that makes it possible to measure the rotation of the light polarization plane in small sections of the sample, it was possible to determine the projection of the resultant magnetic moment of the iron sublattices on the light-propagation direction in the individual domains (the directions of the vectors M_d , $-M_d$, and $M=M_d+M_d$ can be assumed to coincide, since the kink angle of the iron sublattices does not exceed several tenths of a degree at the employed field intensities). By rotating the sample through a small angle about an axis perpendicular to the vectors k and H and by measuring the Faraday rotation of one and the same domain, and also by taking into account the GdIG cubic symmetry, we were able to determine the polar and azimuthal angles of the vector M.

Figure 2 illustrates the change of the Faraday rotation of a small section of the sample, with approximate diameter 75μ , when domains of various types pass through it and the temperature is varied, for two orientations of H. The insert of Fig. 2 (see also the inserts of Figs. 5 and 7 below), the numbers 1, ..., 8 denote the easy-magnetization directions of the type [111]. Small rotations of the sample about the vertical axis produce oppositely directed changes in the Faraday rotation of the different domains, which produce identical rotations of the plane of the polarization when H is exactly oriented along [100] or [111] and lead to a more distinct delineation of the domains, especially when H is close to [100] (Fig. 2a). The directions of the magnetic moments of the sublattices in the chosen domain do not remain constant when the temperature or the field changes.

Different values of H and T correspond to different orientations of M in a domain of the same type, and in this case M_d and M_d lie closer to one of the easy directions, but do not coincide with it. To emphasize this circumstance, the different domain types are numbered $1', \dots, 8'$. Thus for example, in the domain of type $1'$ the easy direction closest to M_d is the direction 1, and the angle between M_d and the direction 1 changes with changing H or T.

In the case when H makes a certain angle α with the high-symmetry axis [100] or [111], the directions of M_d differ, naturally, at the same values of H and T, from the directions of M_d in the case of strict orientation. Emphasizing this circumstance we label the domains in the case $\alpha \neq 0$ by $1'', \dots, 8''$. In the domain of type $1''$, M_d makes the smallest angle with the direction 1, but at the same external parameters H and T the orientation of M_d differs in this case from the orientation of M_d in the domains $1'$ if the field is exactly oriented.

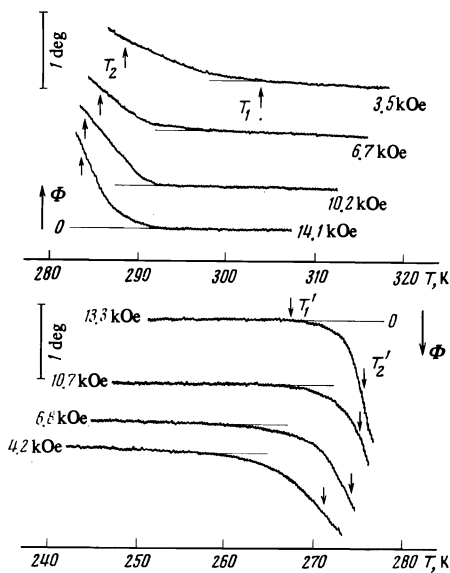


FIG. 3. Temperature dependences of the Faraday rotation of GdIG near the temperatures at which canted magnetic structures appear. The [100] direction makes an approximate angle 0.5° with the vector $H \perp k$; T_1 and T_1' are the temperatures at which Faraday rotation comparable with the noise signals appears, while T_2 and T_2' are the temperatures at which magnetic twins can be visually observed.

By identifying all the domain types it becomes possible to trace visually the positions of their boundaries, owing to the different color hues of the individual domains and of their overlap regions. By fixing the instants of the appearance and of the vanishing of domains of a definite type, we can delineate in the H - T plane the region of the existence of a given magnetic state. We consider below the field orientations $H \parallel [100]$ and $H \parallel [111]$.

1) $H \parallel [100]$. In this case the transition from the collinear to the canted state is smooth, and only the presence of four equivalent planes can lead to the formation of an inhomogeneous state. Furthermore, in a narrow temperature interval, at field intensities lower than critical, first-order phase transitions take place between the noncollinear states, and additional stratification of the sample is possible.^[4,5]

A characteristic feature of the case $H \parallel [100]$ is the presence of a homogeneous smooth rotation of the magnetic moments of the sublattices, preceding the appearance of the domains. At the most accurately possible setting of the field in the (110) plane of the sample, the smooth rotation remains unnoticed down all the way to the temperature at which the domains occur. It appears that this rotation takes place in the sample plane. A deviation of the field direction from the sample plane through a small angle (less than 0.5°) throws the magnetic moments over into another plane and the rotation becomes visible. The sign of the rotation depends on the direction of the deviation of the (110) plane from the vector H . Although the Faraday as a result of the sublattice rotation is noticeable when T_c is approached, starting with the temperatures T_1 and T_1' (Fig. 3), magnetic twins are observed only within the

temperature interval $T_2 T_2'$, which is much narrower than the interval $T_1 T_1'$. Figure 3 shows sections of the temperature dependences of the Faraday rotation corresponding to the appearance of the canted states in GdIG. The figure indicates also the temperatures T_2 and T_2' at which the already formed magnetic twins are visually observable.

The appearance and development of the domain structure are illustrated in Fig. 4. The angle between the analyzer and the polarizer differs somewhat from 90° . The twin formation is noticeable on photographs 1 and 2, viz., the smeared and weak spots on photograph 1 give way to well formed twins in photograph 2, with well defined boundary. As the temperature approaches T_c further, it becomes possible to identify the temperature at which a distinct domain structure appears. Photographs 3-5 show already large twins, penetrating through the entire sample, of type $3'$ (dark) and $1'$

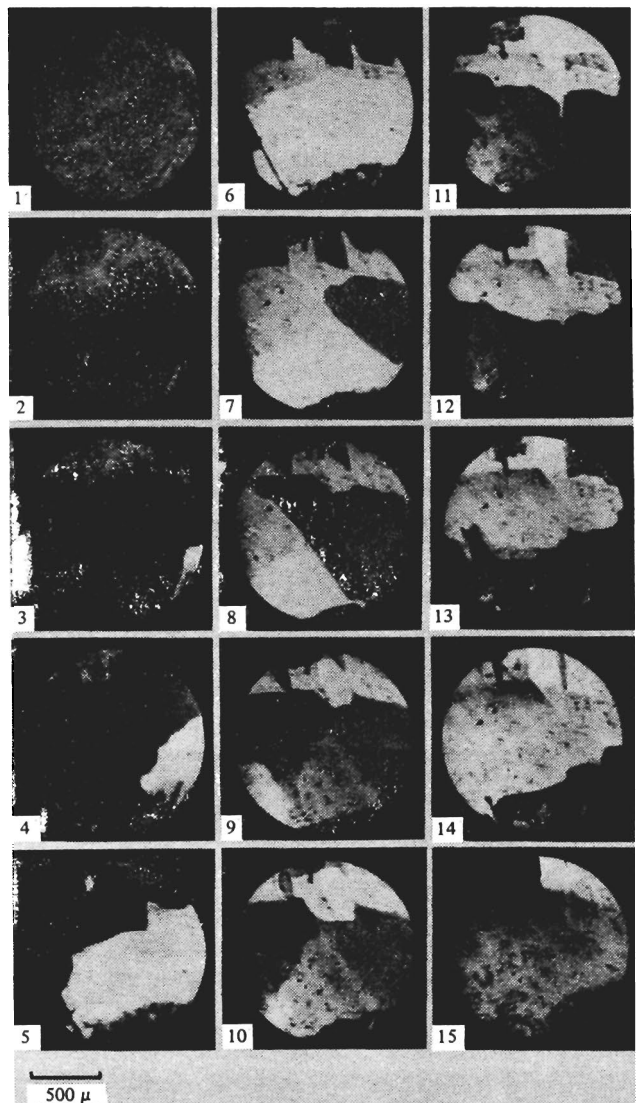


FIG. 4. Field-induced magnetic twins in GdIG near T_c at $H=14.1$ kOe close to [100] in direction; temperature (in $^\circ\text{K}$): 1—275.21; 2—276.45; 3—277.92; 4—278.26; 5—278.82; 6—279.13; 7—279.62; 8—279.75; 9—279.92; 10—280.05; 11—280.29; 12—280.65; 13—280.73; 14—280.87; 15—282.25.

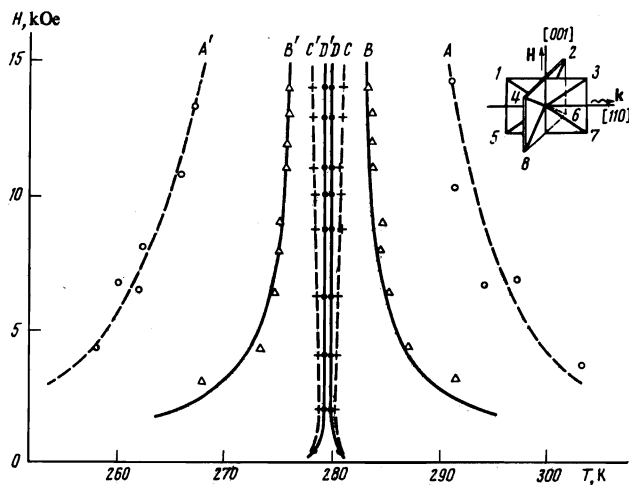


FIG. 5. Diagram of magnetic states of GdIG at $H \parallel [100]$. The regions between lines A and B and lines A' and B' are the regions of approach to the collinear states; lines B and B' are the calculated lines of phase transitions between the collinear and canted states; the regions bounded by lines B' , C' and B , C are the regions of formation of magnetic twins with equivalent magnetic structures; the region bounded by lines D and D' is the region of coexistence of nonequivalent magnetic structures.

(light). Photos 7–9 show clearly the appearance and the growth of a new magnetic phase (domain of type 7') and the vanishing of the former state 1'. The growth of the domain of type 5' is seen in photos 10–15. With further temperature rise, a smooth and uniform rotation of the domains toward the direction of H is observed. Many photographs show in the upper part of the sample a section with immobile boundaries—a block with a somewhat different compensation temperature. The instants of the appearance and of the vanishing of the domains are shifted in temperature in this block in comparison with remainder of the sample.

By determining the temperatures at which various types of domains appear and vanish, we can plot the phase diagram shown in Fig. 5. The dashed lines A and A' show the boundaries of the region within which the canted states are realized. The region of the existence of clearly pronounced domains that penetrate frequently through the entire sample, of the type 1', 2', 3', 4' and 5', 6', 7', 8', is bounded respectively by the lines C' , D and C , D' . The lines D and D' separate the region of existence of nonequivalent magnetic states of the type 1', 2', 3', 4' and 5', 6', 7', 8'. The triangles in the figure show the temperatures T_2 and T_2' at which the just formed magnetic twins become noticeable. The solid lines B and B' drawn near these points are the calculated curves of the second-order phase transitions from the collinear to the canted states.

2) $H \parallel [111]$. In contrast to the preceding case of field orientation, if $H \parallel [111]$ there is no smooth rotation of the sublattices. The process of the reorientation of the moments begins with the appearance of domains in which the directions of the sublattice moments are close to the directions of the equivalent easy axes 2, 3, and 4. The temperature interval in which the interdomain walls are formed is practically nonexistent. The

evolution of the domain picture with changing temperature is shown in Fig. 6. In photo 1 the sample is still homogeneous, photos 2 and 3 show a light noncollinear twin (magnetic moments M_a near the direction 2) and a dark one (moments near direction 3), as well as a section with collinear arrangement of the magnetic moments (gray region of the sample). The canted phases appear in the form of narrow strips and wedges directed along $[111]$. The replacements of the low-temperature canted structures by high-temperature ones (photo 7) and the replacement of the canted structures by a collinear one (photos 11–14) proceed in similar manner.

The diagram of state constructed as a result of the visual observations is shown in Fig. 7. The numbers next to the curves correspond to the types of the appearing or vanishing domains. The dashed lines show the calculated stability limits of the canted structures.

Figure 8 illustrates the onset of a homogeneous mag-

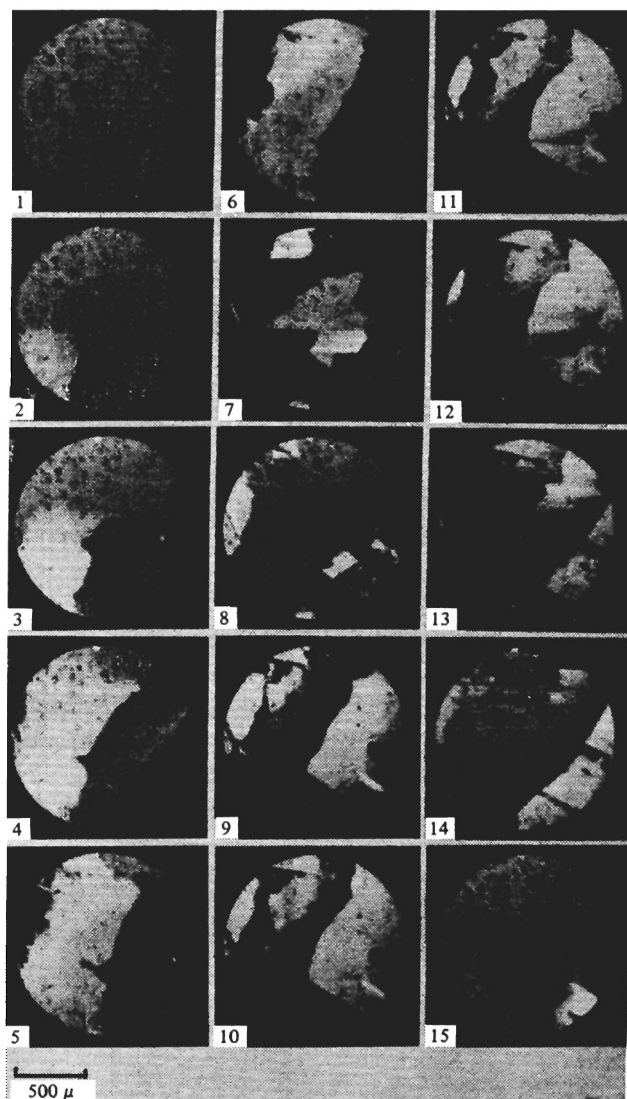


FIG. 6. Field-induced magnetic twins in GdIG near T_c at $H = 14.1$ kOe close in direction to $[111]$. Temperature (in $^{\circ}\text{K}$): 1—277.47; 2—277.98; 3—278.28; 4—278.54; 5—278.67; 6—279.03; 7—279.51; 8—279.72; 9—280.11; 10—280.37; 11—280.56; 12—280.69; 13—280.85; 14—281.03; 15—281.98.

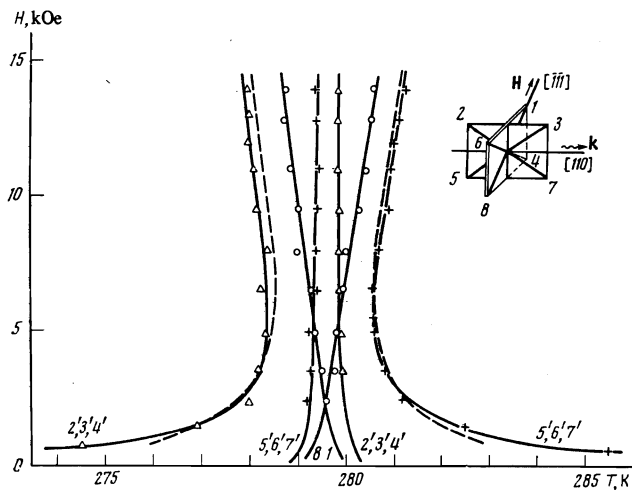


FIG. 7. Diagram of magnetic states of GdIG at $H \parallel [111]$. The numbers at the solid curves correspond to the types of the appearing or vanishing domains. The dashed lines are the calculated stability limits of the canted structures.

netic structure under the influence of a magnetic field at a constant temperature. The magnetic field first magnetizes the sample homogeneously (photo 2), and then (photos 3, 4), inducing a noncollinear structure, the magnetic field leads to the formation of twins and to the coexistence of phases. The collinear phase is observed in the form of horizontal strips.

The change in the relative volume of the coexisting phases and the equivalent structure proceeds via jumpwise as well as smooth motion of the walls. The domain walls between the equivalent structures are frequently observed (Fig. 9, photo 1), and have a width on the order of 1μ . In some cases the walls between

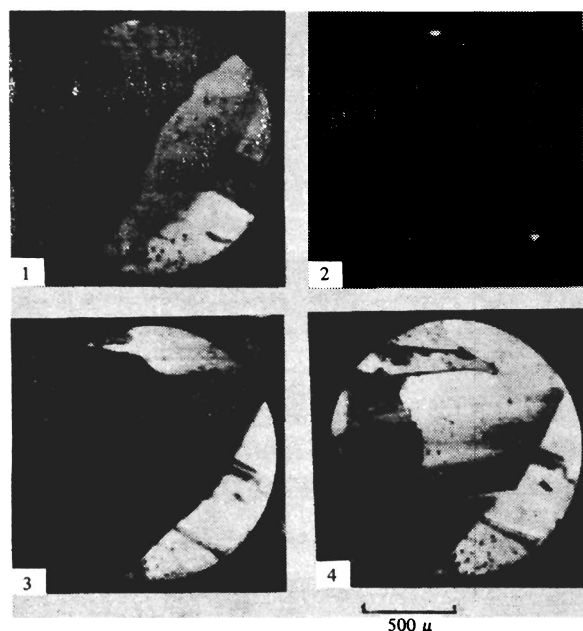


FIG. 8. Onset of a magnetically inhomogeneous state under the influence of a magnetic field at a constant temperature close to T_c ; $T = 280.9^\circ\text{K}$; field intensity (kOe): 1—0.7, 2—7.9, 3—11.3, 4—14.3.

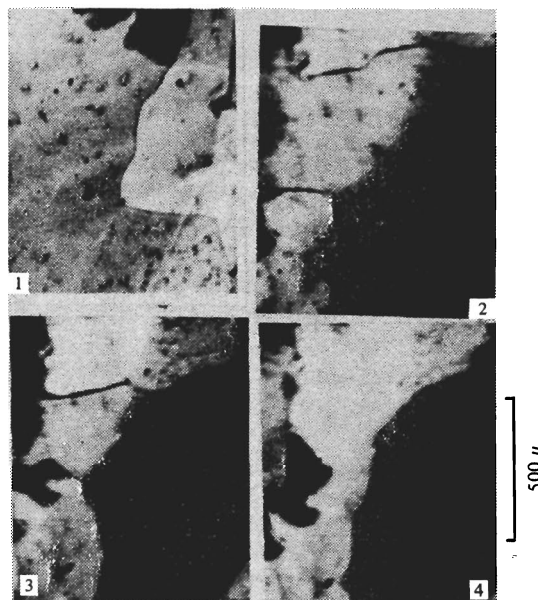


FIG. 9. Boundaries between magnetic twins in a (100) GdIG plate; the polarizers are crossed. Photo 1: $H \parallel [100]$, $H = 14.1$ kOe, $T \approx 280.6^\circ\text{K}$; boundary between magnetic twins of type $5'$ and $7'$. Photos 2-4: $H \parallel [111]$, $H = 14.1$ kOe, the temperature changes uniformly from 280.21 to 280.37°K ; boundaries between the magnetic twins of type $5'$ and $7'$, dark regions—twins of type $6'$.

the twins can serve as nuclei for the formation of a new phase. Photos 2-4 of Fig. 9 illustrate the transformation of a domain wall into a layer, and then into a domain of a new phase. The dark sections on photos 3 and 4 constitute domains in which the magnetic moments lie in the plane of the sample.

DISCUSSION

It follows from the visual observations that in the region of the existence of the noncollinear structure the sample becomes magnetically inhomogeneous and breaks up into sections with energywise equivalent magnetic structures that differ only in the azimuthal angles of the magnetic moments, at one and the same angle between the magnetic moment and the vector H , and at identical resultant magnetic moments. The twin structure in an ideal crystal is energywise not favored, owing to the increase of the energy in the domain wall. It can, however, be kinetically stable.^[6] In addition, an important role in the formation of the inhomogeneous structure can be played by the entropy contribution of the domain walls, the positions of which are not fixed by the demagnetizing fields, in contrast to antiferromagnets.^[7,8] In a real crystal, on the other hand, the lattice and macroscopic defects (say, residual stresses) can cause the magnetically-inhomogeneous states of the sample to turn out to be energywise more favored, owing to the decrease of the elastic energy of the crystal as a result of the magnetically-elastic interaction. The important role of the magnetoelastic interaction is evidenced by the high sensitivity of the form of the domain wall to the stresses of the crystal. It is also typical that twins with magnetic moments that lie in the plane of the sample are rarely encountered. The for-

mation of such domains is energywise unfavored because of the increase of the elastic energy by magnetostriction. On the other hand, the elastically stressed regions cause the boundaries between definite twins to turn sometimes into a layer of variable thickness and can be transformed into a separate domain with $\mathbf{M} \parallel (110)$ (Fig. 9).

The positions of the obtained boundaries of the regions of the existence of various magnetic states of GdIG can be compared with the positions of the stability regions of the magnetic phases. The latter can be constructed by using the results of^[9], in which the molecular-field theory method was used to study the process of breaking of the sublattices in a cubic three-sublattice ferrite. Considering a small temperature region in the vicinities of the compensation temperature $t = (T - T_c)/T_c \ll 1$ and confining ourselves to small magnetic fields $h = H/\lambda M \ll 1$, we can write for the equilibrium values of the sublattice rotation angle θ .

$$\begin{aligned} \mathbf{H} \parallel [100], \quad \cos^3 \theta - \frac{1}{3} \left(1 - \frac{h^2 \alpha}{\kappa \beta} \right) \cos \theta + \frac{m_3'}{3\kappa} h t = 0; \\ \mathbf{H} \parallel [111], \quad h^2 \alpha \cos \theta + h t m_3' \beta + \kappa \beta \left\{ \frac{7}{3} \sin^2 \theta \cos \theta - \frac{4}{3} \cos \theta \right. \\ \left. - \frac{\sqrt{2}}{3} (4 \sin^2 \theta - 3 \sin \theta) \right\} = 0. \end{aligned}$$

Here $\theta = \frac{1}{2}(\theta_1 + \theta_2)$ is the average angle of rotation of the magnetic moments of the iron sublattices, $\kappa = K/\lambda M$, K is the anisotropy constant, λ and λ_{ij} are the exchange constants,

$$\begin{aligned} \alpha = 1 - m_3' \beta + \frac{\lambda - \lambda_{13} - \lambda_{23}}{\lambda_{12}}, \quad \beta = 1 - \frac{\lambda_{13} \lambda_{23}}{\lambda \lambda_{12}}, \quad m_3' = \frac{M_{3k'}}{M_1 - M_2}, \\ M_{3k}' = M_{30} \left(\frac{\partial B(x)}{\partial x} \right)_{T=T_c, H=0}. \end{aligned}$$

In the case $\mathbf{H} \parallel [100]$, the equation for the boundaries of the region of the canted states (lines of second-order phase transition) takes the simple form

$$t_b = - \left(\frac{2\kappa}{m_3' h} + \frac{h\alpha}{m_3' \beta} \right).$$

In the calculation we used the following values of the sublattice magnetic moments^[10,11]: $M_1 = 75.5$ cgs emu/g, $M_2 = 53.3$ cgs emu/g, $M_{30} = 124.4$ cgs emu/g. The ratio β/α was taken equal to 8.9 in accord with^[9], where it was determined from the slopes of the boundaries between the canted and collinear GdIG phases in stronger fields. The magnetic-anisotropy constant was assumed to be $K = -6.7 \times 10^3$ erg/cm³,^[12] and the effective exchange constant $\lambda = 11550$ g/cgs emu was determined from the value $T_c = 285.0$ °K. The exchange field acting on the rare-earth sublattice is $-\lambda(M_1 - M_2) = 2.56 \times 10^5$ Oe, and the reduced anisotropy constant is $\kappa = 1.85 \times 10^{-4}$.

In the case $\mathbf{H} \parallel [100]$, the obtained boundaries pass near the experimental points corresponding to the appearance in the sample of magnetic twins (Fig. 5). The good agreement between the phase boundaries and the experimental points of twin appearances should be regarded as accidental, since the definition of the temperature at which sufficiently abrupt boundaries between the twins is somewhat arbitrary. However, the for-

mation of noncollinear twins near the stability-loss line of the collinear phase is in accordance with the rules. In a wide temperature region between the lines A and B or A' and B', within which, according to calculation, only the collinear state should be realized, the Faraday rotation, which reaches more than 0.1 of the maximum value, indicates nevertheless that a rotation of the sublattices takes place here. It appears that the sublattice rotation in this temperature interval is connected with the existence of microscopic and lattice defects in the sample. It is analogous to the process of the approach of the technical magnetization curve to saturation.^[13,14] The approach of the $\Phi(T)$ curve to zero with increasing distance from T_c carries information on the microscopic crystal defects in the sample. It is of interest in this connection to investigate in greater detail the regularities of the tail of the $\Phi(T)$ curve in the longitudinal and transverse geometries. We note that the transverse experimental geometry is more sensitive to the deviation of the vectors \mathbf{M}_i from the H direction, for in this case $\Phi \sim \sin \theta$. In the longitudinal geometry, on the other hand, both Φ and M are proportional to $\cos \theta$.

The calculated stability loss lines of the canted phases in the case $\mathbf{H} \parallel [111]$ are shown dashed in Fig. 7. They agree well with the experimentally determined boundaries of the region within which the canted magnetic structures are realized. The other experimental data agree well with the results of the investigations in the longitudinal geometry.^[5]

In conclusion, we take the opportunity to thank V. V. Eremenko for interest in the work and for useful discussions, and A. V. Antonov, V. I. Mosel', O. M. Kononov, M. B. Kosmyna, and V. M. Puzikov for supplying the single crystals and the GdIG samples.

¹K. P. Belov, *Ferrity v sil'nykh magnitnykh polyakh* (Ferrites in Strong Magnetic Fields), Nauka, 1972.

²V. V. Eremenko, N. F. Kharchenko, and S. L. Gnatchenko, *Digests of the Intermag Conference, 1974, Toronto, Canada*, 7-7.

³F. V. Lisovskii and V. I. Shapovalov, *Pis'ma Zh. Eksp. Teor. Fiz.* **20**, 128 (1974) [*JETP Lett.* **20**, 55 (1974)].

⁴N. F. Karchenko, V. V. Eremenko, and S. L. Gnatchenko, *Pis'ma Zh. Eksp. Teor. Fiz.* **20**, 612 (1974) [*JETP Lett.* **20**, 280 (1974)].

⁵N. F. Kharchenko, V. V. Eremenko, and S. L. Gnatchenko, *Zh. Eksp. Teor. Fiz.* **69**, 1697 (1975) [*Sov. Phys. JETP* **42**, 862].

⁶I. M. Lifshitz, *Zh. Eksp. Teor. Fiz.* **42**, 1354 (1962) [*Sov. Phys. JETP* **15**, 939 (1962)].

⁷Y. Y. Li, *Phys. Rev.* **101**, 1450 (1956).

⁸M. M. Fartetdinov, *Fiz. Metal. Metalloved.* **19**, 809 (1965).

⁹N. F. Kharchenko, V. V. Eremenko, S. L. Gnatchenko, L. I. Belyi, and E. M. Kabanova, *Zh. Eksp. Teor. Fiz.* **68**, 1073 (1975) [*Sov. Phys. JETP* **41**, 531 (1975)].

¹⁰J. D. Lister and G. B. Benedek, *J. Appl. Phys.* **37**, 1330 (1966).

¹¹E. E. Anderson, *Phys. Rev.* **134**, A1581 (1964).

¹²G. P. Podzigus, H. Meyek, and R. V. Jones, *J. Appl. Phys.* **31**, 3765 (1960).

¹³N. S. Akulov, *Z. Phys.* **69**, 278, 822 (1931).

¹⁴W. F. Brown, Jr., *Phys. Rev.* **82**, 94 (1951).

Translated by J. G. Adashko